Journal of Techniques, ISSN: 2708-8383, Vol. 6, No. 3, 2024, Pages 52-65
DOI: https://doi.org/10.51173/jt.v6i3.1930

JOURNAL OF TECHNIQUES

Journal homepage: http://journal.mtu.edu.iq

RESEARCH ARTICLE - MECHANICAL ENGINEERING

Design and Optimization of Iron Cow Stem with Flaps by Finite Element Method and Genetic Algorithm

Khaled Kamal Oude[1], Ali Adelkhani[1*]

[1]Department of Mechanical Engineering, Kermanshah Branch, Islamic Azad University, Kermanshah, Iran

[*] Corresponding author E-mail: a.adelkhani@iauksh.ac.ir

Article Info.

Article history:

Received
25 August 2023

Accepted
12 March 2024

Publishing
30 September 2024

Abstract

Reversible plows are one of the important and efficient tools in primary tillage, which are affected by many dynamic loads. These tools are damaged in different working conditions, particularly from the stem area. For this reason, in this research, a method based on the finite element method and genetic algorithm was presented to optimize the reversible plow shaft. In this research, two parameters of cross-sectional area and stem curvature were investigated as independent variables. A total of twenty-four different models for the plow shaft were designed in SolidWorks software, FEM software and used Iron Cow Stem. Then, the assorted designs of the stem in the environment of the abacus were loaded, and stress-free occurred in them and were eliminated. Then, using an artificial neural network, a model was presented to estimate the von Mises tension based on the information related to the cross-sectional area and stem curvature, and this model was able to estimate the maximum von Mises tension with 99% accuracy. Then the mentioned model was linked with the genetic algorithm, and it was used to optimize the plow shaft. After selecting the optimized model through the genetic algorithm, the plow shaft was designed again and the tireless stress that occurred in it under the same loading conditions as the previous conditions was eliminated. The results showed that the maximum stress in this model decreased by 6% compared to the previous models, and the best stem design is (Stress (MPa) VonMises=295.2).

Publisher: Middle Technical University

Keywords: Stress; Finite Element; Plow; Genetic Algorithm; Neural Network.

1. Introduction

With the optimization problems becoming more complicated and the lack of optimal efficiency of traditional analytical methods, the need for stronger tools to solve these problems was felt. In addition to problems such as the need for guarantees in terms of derivability and continuity and the possibility of convergence to the local optimum, the time to solve these methods grows exponentially in many problems. In response to this need, meta-exploratory solving algorithms emerged [1]. These methods do not need any derivative information of the problem; with their special operators, they can escape from the local optimum and discover the overall optimum, and the calculation time required in them as the dimensions of the problem increase, it increases linearly or polynomial. Due to the dispersion of these methods in different research and their lack of complete organization, researchers do not have adequate knowledge of the wide range of these algorithms, their mechanisms, and their features, which are discussed in this article. Efforts have been made to optimize several actions to obtain the best result under certain conditions [2] in engineering problems, such as minimization of cost, shortest length, greatest endurance, and best structure. It is considered necessary to mathematically model these aspects and solve them with appropriate methods [3].

Various optimization methods have been introduced according to the type of problem modeling, such as linear or non-linear, constrained or unconstrained, continuous or discrete, etc., such as different types of methods based on linear programming or non-linear programming. Although these methods work properly, they also have obstacles and problems. These methods find the local optimum, especially if the initial guess is near a local optimum. This problem arises from the KKT-stopping condition. Also, each method should be modified according to the formulation of the objective function and constraints. In addition, each of these methods makes assumptions about the nature of the problem that may not be true [4]. Among these assumptions, we can mention derivability, convexity, and continuity. Apart from these disadvantages, the stability time of these methods in A group of optimization problems called NP-hard increases exponentially as the dimensions of m increase. To overcome these challenges, a special group of optimization methods called metaheuristic methods were invented. The term metaheuristic usually refers to a group of methods. Optimization refers to a specific type of undefined problem. The word heuristic is a Greek word and means to know, understand and discover. Metaheuristic in Farsi is similar to the words of these methods that the word research Since these algorithms rely on decisions and principles of probabilistic and random search in many steps of searching for the optimal solution, these methods are also called random search algorithms. Corresponding to these methods, traditional mathematical methods that generally rely on the gradient information of the optimization problem are called exact or analytical methods [5].

The search algorithms use the similarity ratio mechanism to discover the optimal solution. In most of these algorithms, the search starts by creating a number (in some algorithms, one answer) of a random answer within the allowed range of decision variables (control variables). This

set of answers in each of the algorithms has names such as population, group colony, etc. Also, names such as chromosome, ant, particle, etc. are assigned to each of the answers. Then, with operators (relying on a random number generator), a set of new answers is generated. Next, with different methods, answers are selected from the set of past answers and new answers, and this process continues until the stopping criterion is reached [6].

The algorithm has two key parts. The first part is the structure and method of operators to generate new answers. Another, more important part of these algorithms is the selection stage, where the intelligence of the algorithms is applied. The selection stage involves choosing several current answers to apply operators and generate new answers. In the third stage, selection is applied between old answers and new answers. In some references, this stage is called elite selection. By repeating the focus of generating innovative solutions using superior (more worthy) solutions and transferring the worthier ones to the next stage, it is expected that the quality of the solutions will improve in terms of optimality at each stage [7].

Once upon a time, the only jobs in the country were farming and livestock farming, and all family members worked to prepare food; that is, each person produced food for one person. But with the passage of time and the change of circumstances, he started doing other things as well. These conditions required farmers and ranchers to produce other people's food in addition to their food, to the extent that at present, each producer produces food for several hundred people, and this is in line with the growth of the world's population. It is on the rise [8] obvious that the methods and tools of production in the present time are different from the tools and methods of the predecessors. In the beginning, Bashar used to do all the work by hand. But nowadays, different devices and machines are used to produce the food needed by humans. Now, with the increase of the population and to compensate for this increase in demand, the amount of production should be increased. This increase in the amount of production is achieved by removing the obstacles and defects in the work. Improvement of seeds, new planting patterns, fertilizers, pesticides, etc., are some of the things that are used to increase the production rate. Shawarzi's cars are also effective in this field. Inventing new tires and improving the efficiency and working capacity of machines can have a tremendous effect in this direction [9].

At the beginning of the century, the important and effective role of plowing was realized. An operation in which it helped to condition the soil by stirring and creating voids between the soil grains. Among the other advantages of plowing operations, control and prevention of the increase of weeds, destruction of compacted layers of soil, and greater penetration of roots and making them more accessible to collect required materials and water can be mentioned [10] reversible plows are one of the most common tools are plowing and agriculture, which is subject to many failures. Considering the failure of the reversible plow shaft due to static and dynamic forces, the optimization of its shaft can improve the reliability of using this part to some extent [11]. One of the solutions that researchers have taken recently to optimize agricultural tools is the use of finite element models and optimization algorithms. optimize and suggest a suitable model to replace it.

The first tractors were made of external combustion engines with bulky iron wheels. These tractors needed to carry a large amount of water and charcoal or wood as fuel for their engines. With the invention of internal combustion engines, the volume of the engine was much smaller; the crew was reduced to two people, the driver and the assistant driver, but the wheels were iron [12]. and its torque is higher. Recently, gas internal combustion engines that use liquid gas capsules have been mounted on tractors. Early tractors did not have three-point connections, and the implements were pulled along with the tractor. With the invention of the hydraulic system and the connection of Three points, most of the implements were made as mounted or semi-mounted and removing and harrowing were done in the middle of the hydraulic system. By lowering the lever and harrow, it fell to the ground like an iron bull, and if it reached soft soil when plowing, the iron bull went lower, which caused a lot of resistance to the tractor when it hit the hard soil again. This resistance often caused the tractor wheels to slip and sometimes break the tires. To fix the buckling, the driver had to raise the hydraulic lever a little, the iron bull was raised, and then the lever was lowered a little again to reach the initial depth [13]. The hydraulic system of today's tractors is automatic and equipped with two control systems, with six and position control. The old tractors did not have an axle. This shaft is the generator of rotary motion. Today's tractors are generally equipped with this shaft, which can easily use parts of agricultural machines that need rotational movement.

The first tool used to break the soil was a piece of wood. Later, deer horns and animal bones were used. When the metal was discovered, a piece of sharp metal was used to break the soil column. A long time later, man was able to use the power of animals to pull the means of breaking the soil. Around 1000 years before Christ, the first man made a type of iron ox that was used for plowing. 100 years later, an iron cow was made, all of its parts except the souk were made of wood, and its souk was made of metal [14].

In 1756, an iron bull called Sex (ESSEX) was made, which had a decal. In 1798, an iron turning bull, whose basis was partially based on mathematical calculations, was made, and in 1832, an iron bull was made, which was made of steel, and the current iron bulls are an evolved type of it [15,16].

Plow parts include chassis, stem and tines, which have different appearance and usage in each type of plow. The most common type of plow is the lap plow, which includes the following main components [17]. The most important part of the plow is its blade. Each of the branches is connected to a stem. The plow blade is in direct contact with the soil and performs cutting operations, opening the furrow, loosening the soil grains, etc. Its shape corresponds to the way the device works. In other plows, their blades are used; for example, in disc plows, several discs are used instead of a blade [18].

The rods are connected to the iron frame through the stem. Other attachments can be attached to the plow shaft to increase its performance and improve its efficiency. Among these suffixes are prefixes, roots, and measuring wheels [19]. The chassis, which is also called the frame of the iron cow, was a strong skeleton to which the stems of the iron cow were attached and kept it strong. B. A series of appendages are also connected to the chassis of the iron cow [20].

This algorithm is inspired by the group behavior of ants in discovering food. Ants leave pheromones during their food journey. The presence of more pheromones in a path indicates the presence of a rich source of food near that path. By modeling the diffusion process, pheromone tracking and its evaporation by sunlight, the ACO algorithm is completed [21].

In this algorithm, the group behavior of honeybees is used in discovering the food location. The performance of worker bees, guard bees, and queen bees has been modelled. Equivalent to these three types of bees, three types of operators receiving information from the neighborhood in a definite form, receiving information from the neighborhood in a probabilistic form, and searching for new areas (equivalent to a mutation

Nomenclature & Symbols			
ACO	Ant Colony Optimization	BP	Back propagation
CAD	Computer-Aided Design Software	MPa	Mega Pascal
FEM	Finite Element Method	MLP	Multilayer Perceptron Network

in the genetic algorithm) are considered in case of no improvement in the competence in the previous stage [22]. It is presented as a basis for modeling the group movement of fish. It models three random search behaviors: following the general movement of the surrounding fish and following the closest fish to the food source [23].

This algorithm is based on the ability of the human body's immune system to deal with pathogenic agents. In this algorithm, a number of the best antibodies (answers) are selected and new answers are created by applying the mutation operator [24].

This algorithm is proposed by using the mechanism of the sound system of bats in detecting the hunting place, identifying obstacles, and locating the nest in the dark. In terms of optimization structure, each bat updates its speed and position for the best position. Status update, possible and a better position does not necessarily replace a weaker position [25].

This algorithm is based on the theory of natural evolution. Similar to the genetic algorithm, it is based on the mutation and combination operators, but the method of operation and the order of their application are completely different. In addition, it is different from the genetic algorithm in the stage of comparison of new and old populations and selection [26]. It is inspired by the light production and radiation of night insects for activities such as mating, attracting prey, and scaring the enemy. In the presented model, insects with the ability to produce more light (more worthy in the optimization objective function) attract weaker insects according to the photo distance [27].

This algorithm is inspired by a group flight of birds. Each bird in the group follows a simple mobile behavior. Repeating and imitating the successful experience of myself and shadow birds modeling this simple principle led to the creation of one of the simplest and, at the same time, the most widely used object exploration algorithms. In addition, the success of this algorithm (together with the ant colony algorithm) in solving a variety of optimization problems led to the presentation and invention of many meta-exploratory algorithms based on collective intelligence [28].

The genetic algorithm is based on the theory of evolution. It is one of the first and most famous algorithms for object exploration. The main operator of this algorithm is composition. Nevertheless, the jump operator is also useful to prevent premature convergence and falling into the trap of local minima. The smart part of this method is its selection and elite selection stage, which transfers better answers to the next generation at each stage [29].

In terms of design, the most important components of the reversible plow are the reversible plate set and the stem connected to the chassis, and there are many complications in the analysis of the parameters of this set. One of the most important parameters affecting the performance of the plow is the force exerted on its stem. In the conditions of collision with hard obstacles, the shear pin usually acts, but because in the conditions of traditional use of the plow, the shear pin is removed and the stem is welded, so when the stem collides with obstacles, it is severely damaged and will cause disturbance in the plowing operation, so it is necessary and necessary that the stem is designed in such a way that it has the greatest tolerance against tensile and twisting forces.

According to the presented materials, the innovative aspect of this research is the optimization of the reversible plow shaft through the combination of the finite element method and genetic algorithm.

The main goal of the current research is to design and optimize the stem of the iron cow. Modeling of iron cow stem by CAD software and Finite element analysis of plow stem and Determination of optimal stem dimensions by genetic algorithm.

The organization of this manuscript is as follows. Section 2 discusses the finite element analysis. Section 3 describes the types of FEA software. Section 4 discusses the tractor and the three-point hitch. Section 5 discusses the experimental data. Section 6 shows the software implementation. Section 7 describes the analysis in four different loading conditions and the results. Section 8 describes the conclusions.

2. Finite Element

The finite element method, as it is known today, was first presented in an article in 1956 by three researchers named Clogue, Top Turner, and Martin. This article shows the application of the finite element method in trusses and triangular sheets with lying load and is considered one of the key advances in the field of finite element method. The finite element method presented by these researchers is the same method that is used today under the title of the C matrix method for solving structures. The method, together with the increasing development of high-speed digital computers, expanded the use of the finite element method and paved the way for solving more complex problems, including the problems of elastic sheet analysis. After the publication of the results of this article, engineers quickly realized the capabilities of the finite element method. The evolution of the finite element method in the early years of its emergence can be studied in an article published by Klug in 1980 [30]. Field problems such as heat transfer, fluids, etc., can be used; a new chapter was opened in the application of this method. In the late 60s and early 70s, while mathematicians were busy presenting their ideas about topics such as error, there were limits of convergence in the finite element method, engineers and other users of this method were also studying similar topics in the field of solid mechanics. From 1960 onwards, the finite element method gained widespread acceptance in the field of civil engineering. Articles and reference books in this field are increasing day by day [31].

Using the finite element method in a problem requires performing a series of specific steps accurately. For the results obtained from a finite element analysis to be accepted, their accuracy and correctness must be checked. Accuracy means that we must reduce the size of the elements in several steps so that the results are independent of the size of the element. In other words, we must check the convergence of the mesh. For example, you can draw the stress diagram on a certain path, and by making the elements smaller, you can reach a point where there is no change in the diagram [32]. The condition is compared with another finite element analysis. If the results of FEM match with the experimental or

analytical work, its validity is confirmed, and it is confirmed that the modelling has been done correctly. To perform the finite element analysis, a special algorithm should be implemented to solve the problem [33].

At this stage, depending on the type of problem (one-dimensional, two-dimensional, or three-dimensional), the appropriate element is selected, and the body, area, or structure in question is elementizedThe meaning of elementalization of a body is to divide the body or the desired area into a limited number of smaller sections. In a finite element analysis, most of the time is spent on elementing and meshing because the higher the quality of the meshes, the higher the accuracy of the obtained results. When performing finite element analysis with software such as Ansys and Abaqus, meshing is done by the software itself; partitions should only be used in necessary cases to simplify the geometry [34].

The quantity that we want after performing the finite element method (FEM) is measured at the nodes, and it is this value that is considered. For example, in solid mechanics, the field variable is displacement, and in fluid mechanics, velocity. Other quantities in the problem that we are interested in calculating are related to the field variable, and its values are obtained in the nodes and, from there, in the whole body. For example, in solid mechanics, after the displacements of all the nodes have been determined, the relations of strains and stresses at each node can be used to obtain the properties of the entire body. This last step is called post-processing. In the post-processing phase, depending on the desired result or results, the user extracts the desired outputs from the field variable [35].

By specifying the field variable in the previous step, the vector components of the field variable are determined. In each problem, a vector is defined as a general force vector, which shows the effect of external forces or the environment on each element. The stiffness matrix is a matrix that expresses the properties related to the material and the distribution of forces on the nodes of each element. In commercial finite element software such as Nsys and Abaqus, these steps are performed in the software itself. Mechanical engineers, civil engineering, architecture, electricity, industries, and many other disciplines do a lot of their research work with finite element and FEM software [36].

The desired problem is defined for the whole body, not for individual elements, so a general stiffness matrix for the body, as well as a general force vector, must be defined for it. At this stage, by putting together the appropriate components of the German stiffness matrices, the overall German stiffness matrix is formed, and also by arranging the appropriate components related to the German force vectors in the overall force vector, the overall force vector is obtained. Assembling is done automatically in software, but if you write code, this step requires a lot of attention and concentration [37].

Any type of boundary condition (necessary or natural) may be applied on the boundaries of the body or the desired area, but two types of boundary conditions cannot be applied on the same border. To get correct and correct answers, the effect of the boundary conditions applied on the object should be entered in the final stiffness matrix and the general force vector. For example, it is possible in the problems of the mechanics of solids. In some points of the object, the displacements should be zero. Consider a shooting range. In a beam with a single head, it must be prevented from moving in different directions at the place of its support, and rotation should not be allowed at the place of support. Therefore, depending on the problem you are modeling, you must define appropriate boundary conditions. Boundary conditions affect the results and must be properly defined [38].

By applying the boundary conditions in the previous step, we now have a system of equations by solving which the values of the unknown node of the field variable can be calculated. For example, in a problem of mechanics of solids, by solving the final equations, the displacement values of all the nodes are wrong. So far, the steps of performing or applying the finite element method for a problem in general have been completed. In the case of a solid mechanic's problem, another step must be done to complete the solution as follows. In finite element software such as Abaqus, this step is performed by pressing a key by the software itself, and the user does not interfere with it [39].

By obtaining the field variable at the nodes, other quantities that are related to the field variable at the nodes and from there at all points of the body or area can be measured. In a solid mechanic's problem, stresses can be calculated using displacements and strains and then having the strains in hand. Among the famous and powerful software in the field of finite elements are Abaqus and Nsys. In the opinion of Dafid Basheed, the use of the finite element method is especially useful for solving complex problems, and it is easier and less expensive than experimental and analytical methods. Of course, if the modeling is not done in the set and the input software is not given in the set, the output and results will certainly not be correct [40].

3. Design and Optimize the Shank of the Reversible Plow Under Dynamic Loading

This article aimed to design and optimize the shank of the reversible plow under dynamic loading. For this purpose, finite element method and meta-heuristic methods were used. First, the examined models were designed in CAD software, then all the models were analyzed in CAE software, and von Mises stress was eliminated in them. Then, by combining a genetic algorithm and an artificial neural network, the structure of the stem was optimized to withstand the maximum von Mises stress. Fig. 1 shows the flow chart and the process of conducting this research.

3.1. Design of reversible plow

To design the reversible plow and its various components, SolidWorks software was used. At first, in the Part section, the various components of the plow, including the blade, turning plate, screw, and stem, were designed, then these components were assembled in the Assembly environment. In Figs. 2 & 3, the designed model is shown. In Figs. 2-3, the places indicated by A, B, and C show the place where the stem is connected to the chassis of the cover plate and the blade.

To have assorted designs of the plow shaft, changes were observed in two parts of the cross section and the curvature of the shaft. For this purpose, according to Figure 3-3, the cross-section changes were applied to parameters a1 and a2, and for changes in curvature, changes were applied only to c2. For this purpose, the external surface area of the external and internal cross-section of the stem was always constant and equal to 100 cm2 and 64 m2. In Table 1, the changes of a1 and a2, b1 and b2 values are shown. A total of 24 different models of plow shafts were designed, which ranged from 10 to 15 cm in cross-section length and 8 to 5.4 cm in cross-section width. The thickness of the research wall was assumed to be 1 cm in all the models. For the curvature of the stem, the distance c1 was dependent on the outer cross-section, but 6 values were considered for c2. A total of six angles were considered for the stem.

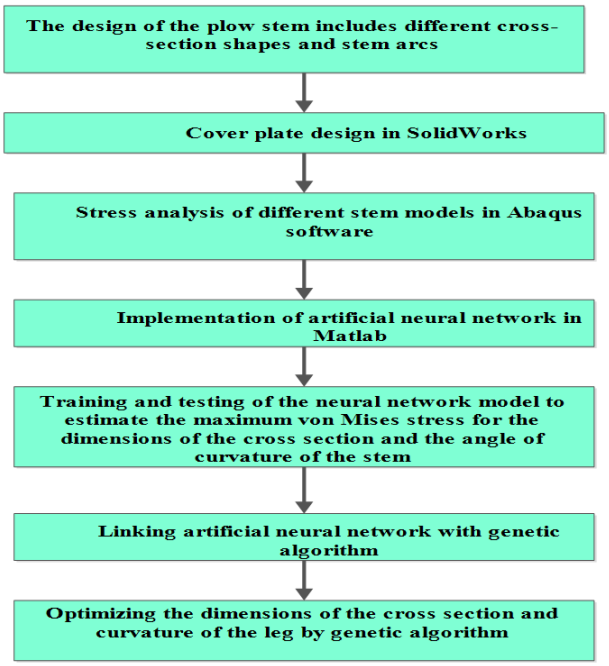

Fig. 1. The workflow of the process

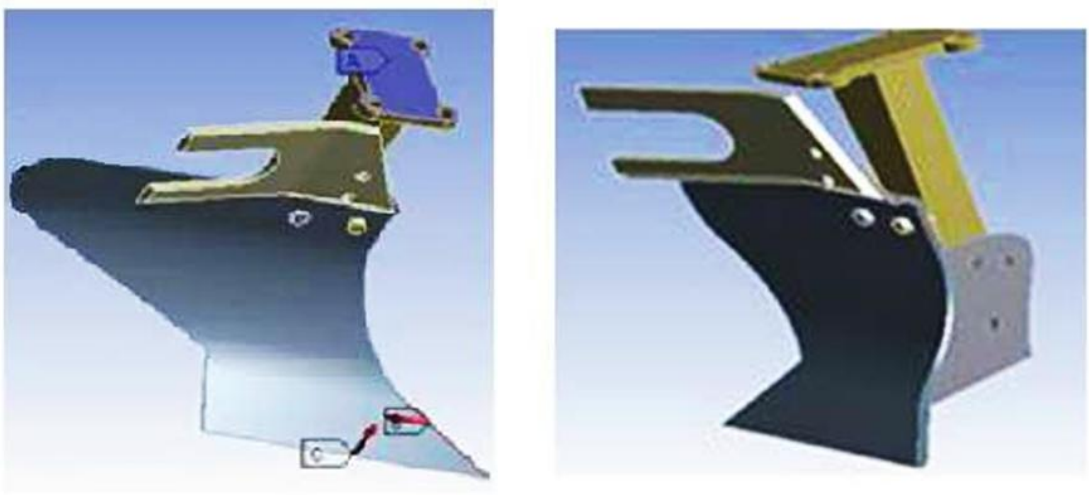

Fig. 2. Two different models of designed plows

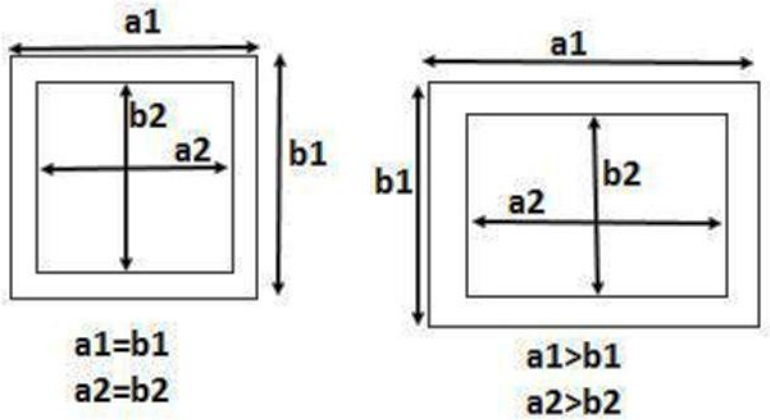

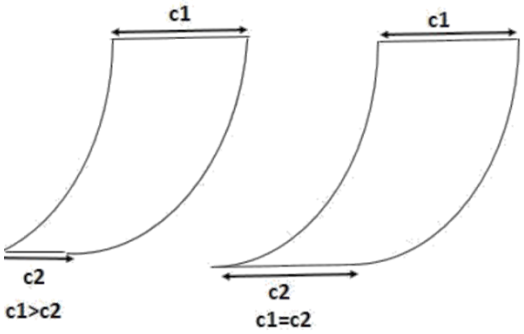

Fig. 3. Different designs for the plow stem

Table 1. Characteristics of a cross section of different models of plow shaft

Row	A1	B1	A2	B2	C1	C2
1	10	10	8	8	10	10
2	10	12	6.35	10	8.25	12
3	10	14	5.15	12	7.15	14
4	10	15	4.47	13	6.67	15
5	9	10	8	8	10	10
6	9	12	6.35	10	8.25	12
7	9	14	5.15	12	7.15	14
8	9	15	4.47	13	6.67	15
9	8	10	8	8	10	10
10	8	12	6.35	10	8.25	12
11	8	14	5.15	12	7.15	14
12	8	15	4.47	13	6.67	15
13	7	10	8	8	10	10
14	7	12	6.35	10	8.25	12
15	7	14	5.15	12	7.15	14
16	7	15	4.47	13	6.67	15
17	6	10	8	8	10	10
18	6	12	6.35	10	8.25	12
19	6	14	5.15	12	7.15	14
20	6	15	4.47	13	6.67	15
21	5	10	8	8	10	10
22	5	12	6.35	10	8.25	12
23	5	14	5.15	12	7.15	14
24	5	15	4.47	13	6.67	15

3.2. Stress analysis of different designs of plow shaft

After 24 different designs were created in the SolidWorks software, it was time to analyze the stress in different samples. The process of stress analysis was conducted using Abaqus finite element software, and for this purpose, the following steps were performed. Before explaining the different steps, it should be mentioned that there are various modules in the Abaqus environment, which include those shown in Fig. 4.

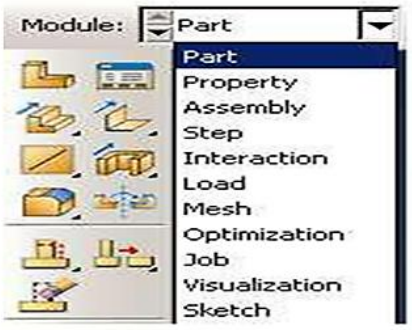

Fig. 4. Different Abaqus modules

3.3. Loading the designed models

All designed samples were saved in .x-t format to be easily loaded into Abaqus2016 software. For this purpose, according to the path shown in Fig. 5, different designs were imported into the Abaqus environment. First, select the File option, then go to the Import section, and after selecting the Model, select the x-t format from the sub-section indicated by number 4.

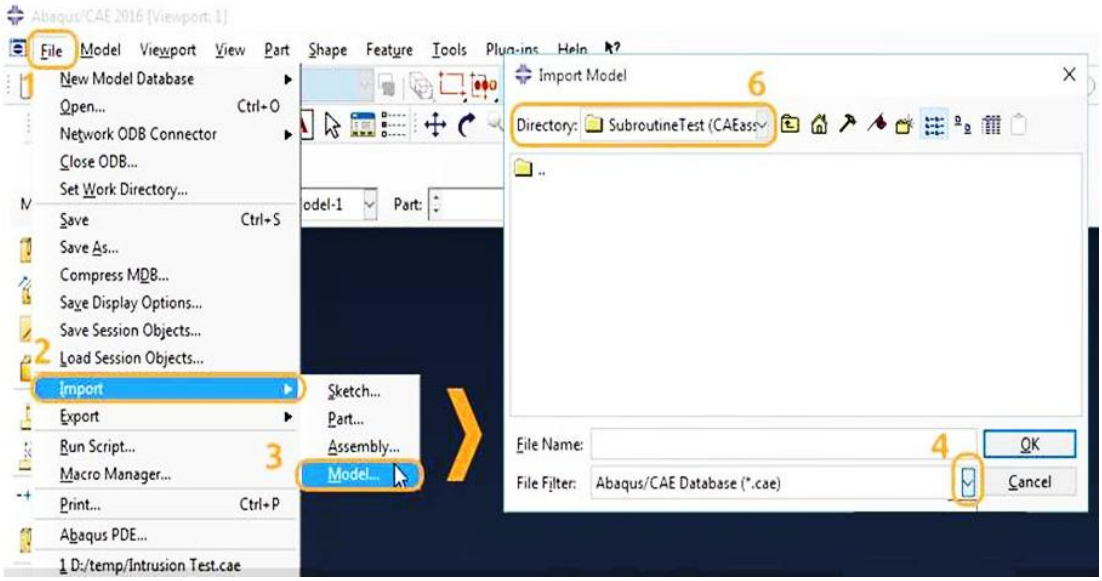

Fig. 5. The Abaqus environment

3.4. Definition of physical and engineering properties

In the Properties module, the physical and engineering properties of various parts of the reversible plow were defined. Considering that the purpose of this research is to compare assorted designs for the stem, all the examined models had the same material for all parts of the plow, such as the stem, blade, and return plate. Its specifications are presented in Table 2.

Table 2. Physical and mechanical characteristics of the materials used in the plow [41]

Physical and mechanical properties	Unit	Amount
Density	g/cm^3	8
Coefficient of elasticity	N/mm^2	210000
Elongation of failure	**%**	22
Yield stress	N/mm^2	235
Ultimate tension	N/mm^2	510
Poisson's ratio	**--**	0.3

3.5. Loading and determining the support for the model

Since the ploughshare is attached to the main chassis, in this research, the upper part of the ploughshare was defined as support. In Fig. 6, the position of the support is represented by A. On the other hand, during tillage operations, the rotary ploughshare is under the influence of two shearing forces to cut the soil and the force caused by turning the soil over. On the other hand, a force caused by turning the soil was applied to the surface of the turning plate, which is shown by C in Fig. 6. It should be noted that both times the attack was defined broadly based on the results presented. In the reference [41], the average of these two forces was reported as 2.5 kN and 3 kN, respectively.

3.6. Meshing and eliminating

The correct solution to a complex mathematical problem will be possible with the help of the finite element method and the correct knowledge of the nature of the problem and the mathematical relationships governing the solution. In the meantime, after choosing the correct solver, the elements should be considered as the most important part of solving a problem in finite elements. Choosing the right type of element, grid size, and several integration points will directly affect the convergence of the solution and reach the desired answer. To mesh the problem, the Mesh module was used, and in this research, the Quad-Dominated element was used for the meshing of the current problem. By default, the priority will be meshing with quadrilateral elements, but in the transitional areas, triangular elements will also be present. In Fig. 7, the meshing is shown.

3.7. Artificial neural network modelling

In this research, to create an intelligent model for diagnosing and predicting the overall stress level in the Khish Gawahan complex, a multilayer perceptron network (MLP) was used. This network includes an input layer, one or more hidden layers, and an output layer. The backpropagation 1 (BP) algorithm is usually used to train this network. During the training of the MLP network with the help of the BP learning algorithm, first, the calculations are performed from the input of the network to the output of the network, and then the estimated error values are propagated to the previous layers. In this method, the Levenberg-Marquardt (LM) algorithm was usually used to update the weights of the artificial neural network. It became one of the most widely used algorithms because it allows for quick network training and minimizes the existing error level.

As mentioned earlier, the MLP network was used in this research. The error backpropagation learning rule and sigmoid function were used in the hidden layer, and the output of the network with 10 neurons in the hidden layer. The inputs of the neural network were different values related to the design of the stem, which included the values of c2, c1, b2, a2, b1, and a1, and its output was the amount of total stress (Von Mises) in the stem. Sixty-four different models were modelled in Abaqus software. In this research, first, the model inputs were standardized, and then the network structure was determined by estimating the overall stress. 70% of the total data was used for neural network training, and

the remaining 30% was used for network testing and evaluation. To train the MLP artificial neural network, three training algorithms were used: Bayesian Regularization, Levenberg-Marquardt, and Scaled Conjugate Gradient [42].

Table 3 shows the range of changes in design parameters. To choose the optimal dimensions for the stem to withstand the most stress, the range of each parameter was divided into 11 parts. That is, in this section, there are 5 parameters, each of which has 11 different values and must be optimized by genetic algorithm and neural network. Due to the limitation in modeling the khish stem to calculate stress, in this research, using 64 primary models and the amount of stress calculated from them, an artificial neural network was implemented to predict the overall stress level in the khish stem. In this section, we want to predict the most optimal dimensions to have the lowest overall stress using the artificial neural network model and genetic algorithm.

3.8. How to display chromosomes

Chromosome length is equal to the total number of different values for each parameter. When the 'iam' gene is equal to one, it indicates that the 'iam' parameter is selected, and when the 'iam' gene is equal to zero, it means that the 'iam' parameter is not selected. A set of chromosomes is called a population. In this research, the shape of different chromosomes, each of which represents a parameter of the stem, was investigated. The program is written in such a way that each chromosome can only transfer one gene. Different chromosomes are shown in Table 3. It should be noted that only one gene from each chromosome was selected at each stage.

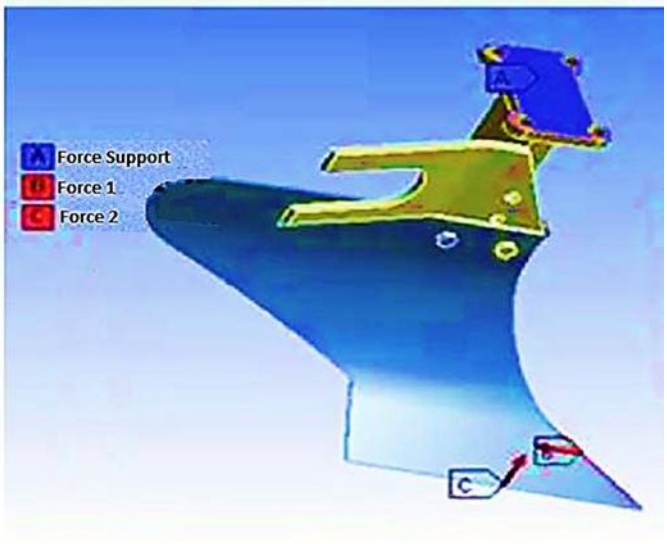

Fig. 6. Determining the place of application of force and support in the reversible plow

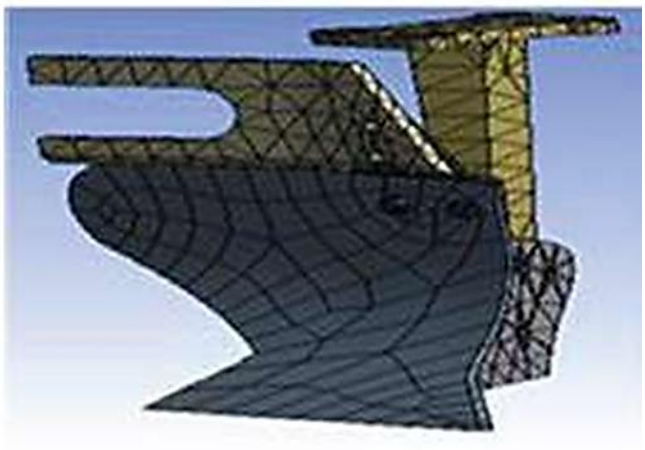

Fig. 7. Meshing of Khish with Quad-Dominated Element

Table 3. Different chromosomes for different parameters of khish stem Chromosome c2

5	5.5	6	6.5	7	7.6	8	8.5	9	9.5	10
Chromosome a1										
10	10.5	11	11.5	12	12.5	13	13.4	14	14.5	15
Chromosome a2										
8	8.5	9	9.5	10	10.5	11	11.5	12	12.5	13
Chromosome b1										
6	6.4	6.8	7.2	7.6	8	8.4	8.8	9.2	9.6	10
Chromosome b2										
4.5	4.4	4.8	5.2	5.6	6	6.4	6.8	7.2	7.6	8

4. Result Analysis

The answers obtained from solving a problem by the finite element method always depend on the size of the mesh and the size of the elements used. By increasing the density of the mesh, the numerical solution of the problem converges into a single solution. Of course, the finer mesh increases the hardware power used to solve the finite element model, and the processing process takes more time. In the case where negligible changes are obtained in the solution results by successively reducing the size of the elements, it is said that "the mesh has converged." Fig. 8 shows the convergence between the response of the analysis and the number of meshes of each model. From 3600 meshes onwards, the changes in maximum stress that occurred in Khish were very small, so this number of elements was considered a criterion for all models.

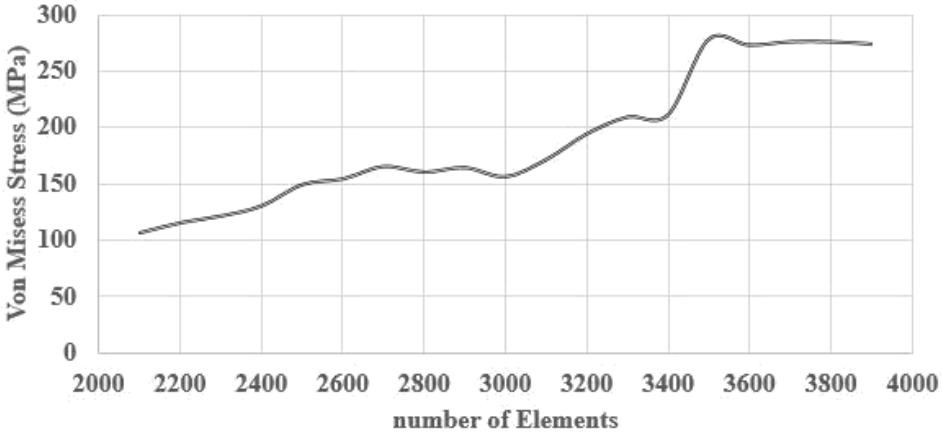

Fig. 8. Convergence in meshing

4.1. Results of stress analysis

The results of stress analysis in different designed models are presented. Table 4 shows the results of stress analysis for different models. Examining the results of Table 4 showed that the maximum von Mises stress in the straw changed with the change in the stem shape. Among the examined models, the maximum von Mises stress was observed for a rectangular section with a stem with the least curvature, and the minimum von Mises stress was observed in a stem with a square section and the most curvature in the stem, which values were 295.2 MPa and 250 MPa, respectively. It was a skunk. Examining the results of their analysis showed that the difference between the minimum and maximum stress that occurred in the set of stems and stems is about 15%. In this research, we intend to reduce the maximum stress by optimizing the dimensions of the stem, or in other words. Increase the safety factor of the stem. In the results, the minimum and maximum stress distribution in Khish per heart is shown in Fig. 8.

Table 4. Von Mises stress values created in Khish according to different stem designs

A1	B1	A2	B2	C2	Stress (MPa) VonMises
10	10	8	8	10	273.5
12	8.25	10	6.35	10	279.6
14	7.15	12	5.15	10	287.9
15	6.67	13	4.47	10	295.2
10	10	8	8	9	275.6
12	8.25	10	6.35	9	280.1
14	7.15	12	5.15	9	286.7
15	6.67	13	4.47	8	290.3
10	10	8	8	8	271.7
12	8.25	10	6.35	8	276.3
14	7.15	12	5.15	8	281.4
15	6.67	13	4.47	7	283.4
10	10	8	8	7	263.9
12	8.25	10	6.35	7	268.2
14	7.15	12	5.15	7	273
15	6.67	13	4.47	6	277.6
10	10	8	8	6	257.3
12	8.25	10	6.35	6	260.4
14	7.15	12	5.15	6	265.6
15	6.67	13	4.47	**5**	270.8
10	10	8	8	5	250
12	8.25	10	6.35	5	254.5
14	7.15	12	5.15	5	261.5
15	6.67	13	4.47	5	267.1

Fig. 9 Maximum and minimum stress occurred in the spike and stem set under the influence of the same loading**.** Examining and analyzing the results showed that the squarer the cross-section of the stem, the lower the maximum stress. In other words, the amount of maximum stress that

occurred in rectangular sections with a greater length-to-width ratio was more than in the sections with a length-to-width ratio of one. Also, the results of the stress analysis showed that as the engine of the plow shaft became thinner, the amount of tension that occurred in the plow assembly decreased, which is also the reason for the shortening of the torque arm of the shaft.

4.2. The results of an artificial neural network to predict the maximum stress

To model and predict the overall stress in the Khish collection, 64 data samples were used. 70% of the total data was used in the training phase and the rest of the data was used to validate the network. Three training algorithms, Bayesian Regularization, Levenberg-Marquardt and Scaled Conjugate Gradient, were used to train the MLP artificial neural network, and the Levenberg-Marquardt method with the lowest error value and the highest correlation was selected as the appropriate algorithm in the training data. Bias shows the difference between the measured output parameter and the predicted value, the closer it is to zero, the higher the efficiency of the model. Finally, the trial and error method was used to determine the architecture of this network. The optimal architecture chosen for this network had 5 neurons in the input layer, 12 neurons in the hidden layer and one neuron in the output layer [44].

The error changes for the training and test data for the Levenberg-Marquardt training algorithm are shown in Figure 9. By repeating the training step in each step, the neural network training error has been reduced for the test and training data, which shows the convergence of the neural network model training towards a constant error rate.

The regression analysis between the predicted outputs and the measured data is presented for the training data in Fig. 10 and the test data in Fig. 11. The existence of high correlation values, bias and low MSE in the training and test stages of the network indicate the optimal performance of the neural network model in estimating the overall stress.

The histogram of the error value by the artificial neural network in predicting the von Mises stress is shown in Figure 12. The highest frequency of error in this case is for values less than 1%. In general, the modelled neural network is a suitable and reliable method for predicting the maximum stress in the stem. According to the results presented in this section, a multi-layer artificial neural network was modelled with Levenberg-Marquardt learning algorithm with five inputs and 12 neurons in the hidden layer with 99.88% accuracy to estimate the overall tension in the Khish complex.

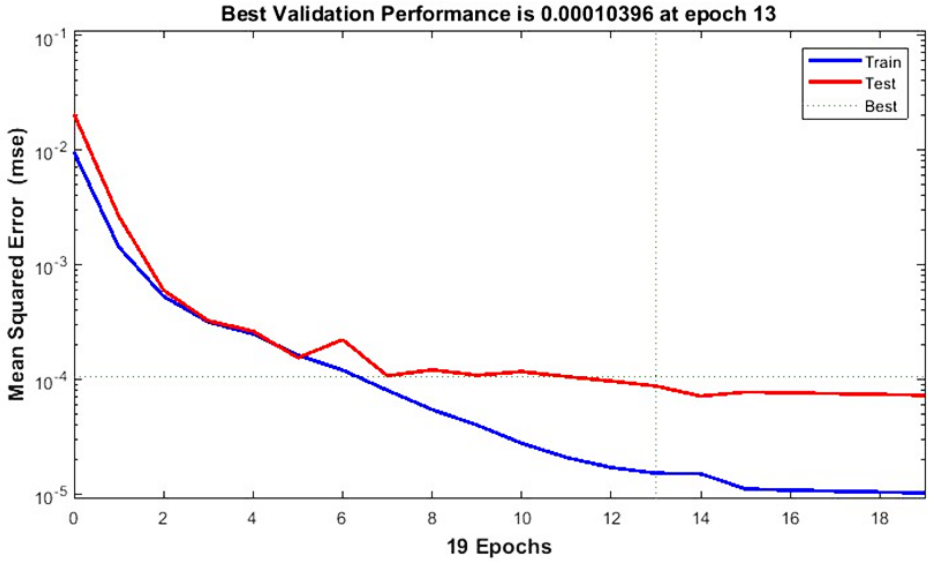

Fig. 9. Error changes for training and test data

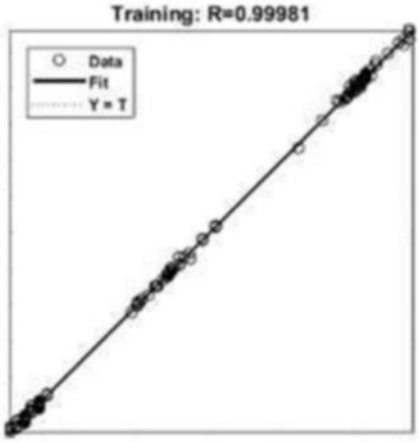

Fig. 10. Regression analysis between predicted stress and actual stress for training data

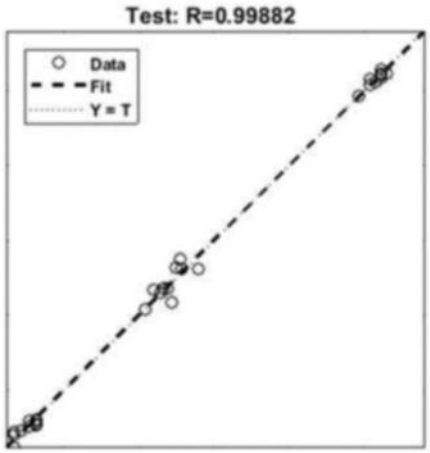

Fig. 11. Regression analysis between predicted stress and actual stress for test data

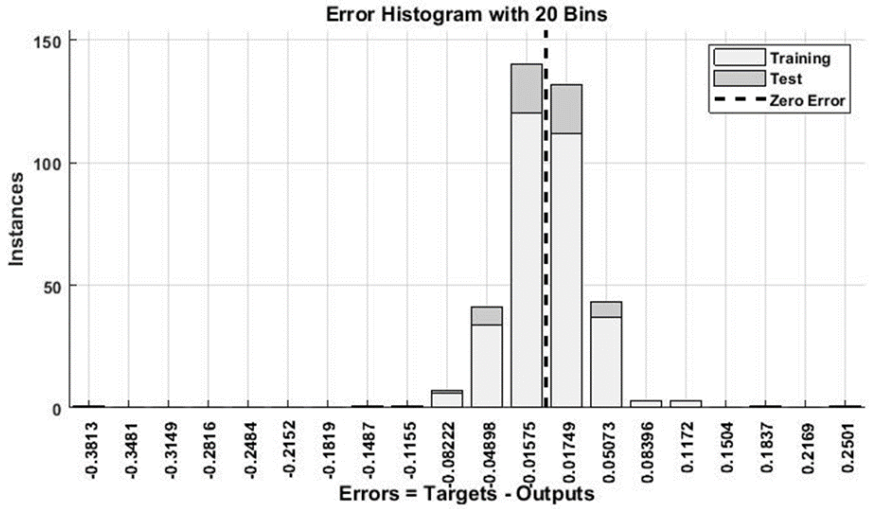

Fig. 12. Histogram of Von Mises stress prediction error by neural network

4.3. Optimization results by ANN-GA

The implemented model of the artificial neural network was implemented for 64 samples, which were calculated by the Abaqus software, the maximum stress of the Khish collection. By linking the artificial neural network with the genetic algorithm, it was used to select the most optimal dimensions of the stem to have the minimum value of the objective function. The output results of the genetic algorithm to minimize the objective function are presented in Fig. 13. As it is clear in the figure, the lowest amount of Von Mises stress in the set of stem and shoot equal to 230.2 MPa was obtained, which was observed as a result of the 40th population of the genetic algorithm. The values of the minimum stress parameters in the set of stems and shoots for c2, a1, b1, a2 and b2 parameters were observed to be equal to 5, 10, 10, 8 and 8 cm, respectively. In the following, the model of the Khish stem was designed according to the above parameters and the stress was analysed again [45].

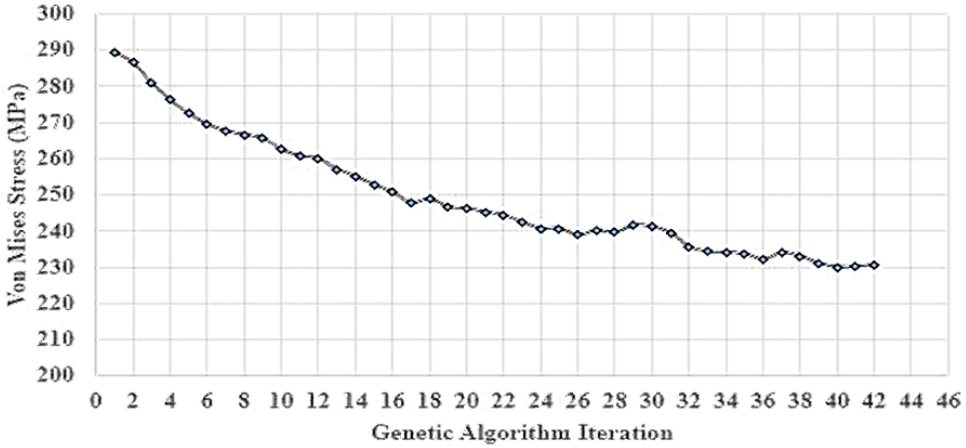

Fig. 13. The final Koon-Mises stress in the good set for different iterations in the genetic algorithm

4.4. Stress analysis of the optimized model

Fig. 14 shows the results of the stress analysis in the stem and tiller of the reversible plow optimized by the genetic algorithm. In this case, the maximum von Mises stress of 233.4 MPa was obtained, which was about 2% higher than the value predicted by the artificial neural network. In any case, the optimization results showed that by using the genetic algorithm and re-designing the reversible plow shaft, the von Mises stress occurring in the joint of the plow shaft and the plow can be reduced from 250 MPa to 233.4 MPa. The results of this research showed that by using the genetic optimization algorithm and neural network, the plow shaft can be designed in such a way that the von Mises stress occurring in the set is reduced by 6.64%. Also, the examination of Fig. 14 showed that, in this case, the maximum stress distribution did not occur in the stem area, and the maximum stress occurred at the blade and blade tip [46].

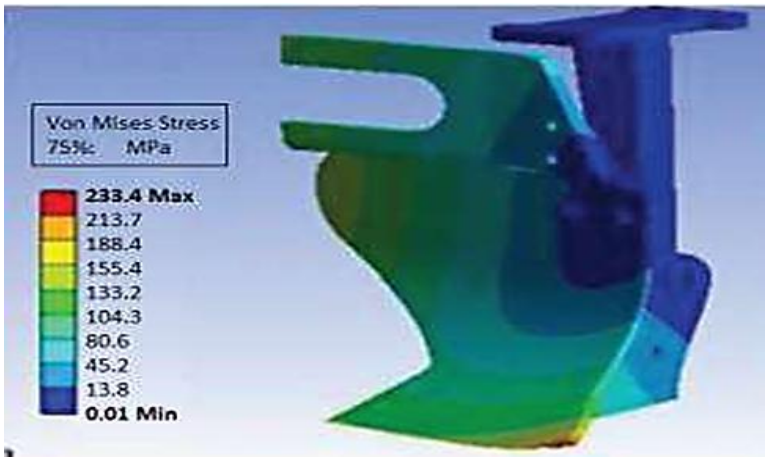

Fig. 14. The stress analysis of stem and cane optimized by genetic algorithm

5. Conclusion

In this study, the reversible plow stem was optimized by genetic algorithm and finite element method. For this purpose, 24 different design models and maximum von Mises stress were calculated in them. Then, it was optimized by using the combination of artificial neural network and genetic algorithm, and the following results were obtained:

- The results of stress analysis for 24 designed models showed that the minimum and maximum stress that occurred were 250 and 290 MPa, respectively.
- The results of the design of different cross-sections of the plow shaft showed that the closer the cross-section of the plow shaft is to the square, the maximum stress occurring in the shaft will decrease.
- The results showed that the closer the ratio of the length to the cross-section of the stem is to one, the better the stem can bear the load.
- The results of examining the curvature of the stem showed that the more the stem tends to be perpendicular to the ground, the less tension occurs in it, and the more the curvature of the stem increases, the less tension will be observed in the stem.
- The results of the estimation of the maximum stress occurred in the khish set by the neural network showed that this model can estimate the maximum von Mises stress with a high accuracy of 99% based on the basic information related to the cross-sectional area of the khish stem.
- The results of plow stem optimization by combining neural network and genetic algorithm reduced the maximum von Mises stress in the set of plow and stem by 19%.
- With the optimization of the plow shaft, not only was the stress reduced, but the plow shaft was under much less stress than in other previous models.

Acknowledgment

The authors sincerely thank all the researchers who supported us, Islamic Azad University, Kermanshah Branch, Department of Production and Manufacturing, Suwaira Technical Institute, Middle Technical University.

References

[1] Y. Liu et al., “Bionic design of thin-walled tubes inspired by the vascular structure of bamboo,” Thin-Walled Structures, vol. 186, p. 110689, May 2023, doi: 10.1016/j.tws.2023.110689.
[2] Q. Zhang et al., “Advanced biomaterials for repairing and reconstruction of mandibular defects,” Materials Science and Engineering: C, vol. 103, p. 109858, Oct. 2019, doi: 10.1016/j.msec.2019.109858.
[3] H. Quan, A. Pirosa, W. Yang, R. O. Ritchie, and M. A. Meyers, “Hydration-induced reversible deformation of the pine cone,” Acta Biomaterialia, vol. 128, pp. 370–383, Jul. 2021, doi: 10.1016/j.actbio.2021.04.049.
[4] R. Sarkar, B. Chen, M. E. Fitzpatrick, D. Fabijanic, and T. Hilditch, “Additive manufacturing-based repair of IN718 superalloy and high-cycle fatigue assessment of the joint,” Additive Manufacturing, vol. 60, p. 103276, Dec. 2022, doi: 10.1016/j.addma.2022.103276.
[5] A. P. More, “Flax fiber–based polymer composites: a review,” Advanced Composites and Hybrid Materials, vol. 5, no. 1, pp. 1–20, May 2021, doi: 10.1007/s42114-021-00246-9.
[6] X.-M. Chen, X. Wang, and Z. Hou, “Editorial: MSC-derived exosomes in tissue regeneration,” Frontiers in Cell and Developmental

Biology, vol. 11, Sep. 2023, doi: 10.3389/fcell.2023.1293109.
[7] I. A. Alhassan, "Land-Use Conflicts between Settler Farmers and Nomadic Fulani Herdsmen in the Kwahu North District, Ghana," Contemporary Journal of African Studies, vol. 4, no. 2, p. 127, Jun. 2017, doi: 10.4314/contjas. v4i2.5. [Online]. Available, doi:10.4314/contjas. v4i2.5
[8] M. Dettinger, A. Wilson, and G. McGurk, "Keeping Water in Climate-Changed Headwaters Longer," San Francisco Estuary and Watershed Science, vol. 21, no. 4, Dec. 2023, doi: 10.15447/sfews.2023v21iss4art1.
[9] S. Duncan Stephens, E. J. Flaherty, W. J. Sutton, W. N. MacDonald, and B. J. Shelp, "Further optimization of macronutrient delivery for subirrigated greenhouse-grown chrysanthemums: calcium and magnesium," Canadian Journal of Plant Science, vol. 101, no. 1, pp. 129–134, Feb. 2021, doi: 10.1139/cjps-2020-0117.
[10] T. Knežić, L. Janjušević, M. Djisalov, S. Yodmuang, and I. Gadjanski, "Using Vertebrate Stem and Progenitor Cells for Cellular Agriculture, State-of-the-Art, Challenges, and Future Perspectives," Biomolecules, vol. 12, no. 5, p. 699, May 2022, doi: 10.3390/biom12050699.
[11] H. A. Ariyanta, S. Chodijah, F. Roji, A. Kurnia, and D. O. B. Apriandanu, "The role of Andrographis paniculata L. modified nanochitosan for lamivudine encapsulation efficiency enhancement and in vitro drug release study," Journal of Drug Delivery Science and Technology, vol. 67, p. 103016, Jan. 2022, doi: 10.1016/j.jddst.2021.103016.
[12] F. V. Hladkykh, "Macroscopic assessment of protective effect of cryopreserved placenta extract in ibuprofen-induced gastroenterocolonopathy," GASTROENTEROLOGY, vol. 55, no. 3, pp. 172–179, Jan. 2022, doi: 10.22141/2308-2097.55.3.2021.241587.
[13] X. Li, H. Shi, K. Pan, M. Dai, W. Wei, and X. Liu, "Improved biocompatibility and antibacterial property of zinc alloy fabricated with γ-polyglutamic acid-g-dopamine/copper coatings for orthopedic implants," Progress in Organic Coatings, vol. 173, p. 107215, Dec. 2022, doi: 10.1016/j.porgcoat.2022.107215.
[14] A. Wei, R. Al-Ameri, M. Y. J. Tan, Y.-C. Koay, and X. Hu, "Effectiveness of carbon fiber-reinforced polymer as a triple-functional material for sustainable protection of reinforced concrete structures," Innovative Infrastructure Solutions, vol. 8, no. 6, May 2023, doi: 10.1007/s41062-023-01139-0.
[15] Y. R. Kang, "Rewriting The Wonderful Wizard of Oz: African American Musical Theatre and The Wiz Live!," The Journal of Modern English Drama, vol. 35, no. 2, pp. 5–30, Aug. 2022, doi: 10.29163/jmed.2022.8.35.2.5.
[16] M. Lendraitis, "Investigation of performance gains on a sailplane with morphing wing trailing edge," Mechanics, vol. 25, no. 4, pp. 299–303, Aug. 2019, doi: 10.5755/j01.mech.25.4.22325.
[17] Z. Su and L. Shao, "A three-dimensional slope stability analysis method based on finite element method stress analysis," Engineering Geology, vol. 280, p. 105910, Jan. 2021, doi: 10.1016/j.enggeo.2020.105910.
[18] K. Jegadeesan and S. Datta, "Design of laminated composite plate for optimum ballistic impact resistance: A finite element approach," Materials Today: Proceedings, vol. 68, pp. 2493–2497, 2022, doi: 10.1016/j.matpr.2022.09.182.
[19] Yu, Hui, Lingling Zheng, Jikuan Qiu, Jiayue Wang, Yaoke Xu, Baoshi Fan, Rui Li, Junxiu Liu, Chao Wang, and Yubo Fan. "Mechanical property analysis and design parameter optimization of a novel nitinol nasal stent based on numerical simulation." Frontiers in Bioengineering and Biotechnology 10, 1064605, 2022, doi:10.3389/fbioe.2022.1064605.
[20] Ge-Zhang, Shangjie, Mingbo Song, Zehang Huang, Maodan Li, and Liqiang Mu. "Comparison and optimization: research on the structure of the PET bottle bottom based on the finite element method." Polymers 14, no. 15, 3174, 2022, doi:10.3389/fbioe.2022.1064605.
[21] T. He, "Extending the cell-based smoothed finite element method into strongly coupled fluid–thermal–structure interaction," International Journal for Numerical Methods in Fluids, vol. 93, no. 4, pp. 1269–1291, Oct. 2020, doi: 10.1002/fld.4928.
[22] H. Boudounit, M. Tarfaoui, and D. Saifaoui, "Fatigue analysis of wind turbine composite blade using finite element method," Wind Engineering, vol. 47, no. 3, pp. 706–721, Feb. 2023, doi: 10.1177/0309524x231155549.
[23] F. Ruggiero et al., "Finite element method for the design of implants for temporal hollowing," JPRAS Open, vol. 32, pp. 18–23, Jun. 2022, doi: 10.1016/j.jpra.2021.12.001.
[24] E. Demir, G. Yalçın, A. Kalaycı, and H. Sağlam, "Biomechanical evaluation of caudally and buccally screwed customised reconstruction plates for lateral segmental defects of mandible," British Journal of Oral and Maxillofacial Surgery, vol. 59, no. 8, pp. 928–934, Oct. 2021, doi: 10.1016/j.bjoms.2020.10.017.
[25] T. Bagherpoor and L. Xuemin, "Structural Optimization Design of 2MW Composite Wind Turbine Blade," Energy Procedia, vol. 105, pp. 1226–1233, May 2017, doi: 10.1016/j.egypro.2017.03.420.
[26] R. Kadge, "Finite Element Analysis on Design Optimized Bevel Gear Pair to Check Its Durability," SAE International Journal of Passenger Vehicle Systems, vol. 15, no. 1, Mar. 2022, doi: 10.4271/15-15-01-0005.
[27] Z. Zhang et al., "Space deployable bistable composite structures with C-cross section based on machine learning and multi-objective optimization," Composite Structures, vol. 297, p. 115983, Oct. 2022, doi: 10.1016/j.compstruct.2022.115983.
[28] M. Ben Jaber, H. Smaoui, and P. Terriault, "Finite element analysis of a shape memory alloy three-dimensional beam based on a finite strain description," Smart Materials and Structures, vol. 17, no. 4, p. 045005, May 2008, doi: 10.1088/0964-1726/17/4/045005.
[29] T. Long, C. Huang, D. Hu, and M. Liu, "Coupling edge-based smoothed finite element method with smoothed particle hydrodynamics for fluid structure interaction problems," Ocean Engineering, vol. 225, p. 108772, Apr. 2021, doi: 10.1016/j.oceaneng.2021.108772.
[30] C. R. Vindigni, G. Mantegna, A. Esposito, C. Orlando, and A. Alaimo, "An aeroelastic beam finite element for time domain preliminary aeroelastic analysis," Mechanics of Advanced Materials and Structures, vol. 30, no. 5, pp. 1064–1072, Sep. 2022, doi: 10.1080/15376494.2022.2124333.
[31] D. D. Angela and M. Ercolino, "Finite Element Analysis of Fatigue Response of Nickel Steel Compact Tension Samples using ABAQUS," Procedia Structural Integrity, vol. 13, pp. 939–946, 2018, doi: 10.1016/j.prostr.2018.12.176.
[32] S. E. F. Huys, A. Van Gysel, M. Y. Mommaerts, and J. V. Sloten, "Evaluation of Patient-Specific Cranial Implant Design Using Finite Element Analysis," World Neurosurgery, vol. 148, pp. 198–204, Apr. 2021, doi: 10.1016/j.wneu.2021.01.102.
[33] P. Ruf et al., "Towards mechanobiologically optimized mandible reconstruction: CAD/CAM miniplates vs. reconstruction plates for fibula free flap fixation: A finite element study," Frontiers in Bioengineering and Biotechnology, vol. 10, Nov. 2022, doi: 10.3389/fbioe.2022.1005022.
[34] A. S. Escalera Mendoza, S. Yao, M. Chetan, and D. T. Griffith, "Design and analysis of a segmented blade for a 50 MW wind turbine rotor," Wind Engineering, vol. 46, no. 4, pp. 1146–1172, Jan. 2022, doi: 10.1177/0309524x211069393.
[35] K. Aggarwal, S. Wu, and J. Papangelis, "Finite element analysis of local shear buckling in corrugated web beams," Engineering Structures,

vol. 162, pp. 37–50, May 2018, doi: 10.1016/j.engstruct.2018.01.016.
[36] A. Borgia et al., "Swept-Source Optical Coherence Tomography-Based Biometry: A Comprehensive Overview," Photonics, vol. 9, no. 12, p. 951, Dec. 2022, doi: 10.3390/photonics9120951.
[37] P. Bortolotti, N. Johnson, N. J. Abbas, E. Anderson, E. Camarena, and J. Paquette, "Land-based wind turbines with flexible rail-transportable blades – Part 1: Conceptual design and aeroservoelastic performance," Wind Energy Science, vol. 6, no. 5, pp. 1277–1290, Sep. 2021, doi: 10.5194/wes-6-1277-2021.
[38] E. Fatehi, H. Yazdani Sarvestani, B. Ashrafi, and A. H. Akbarzadeh, "Accelerated design of architectured ceramics with tunable thermal resistance via a hybrid machine learning and finite element approach," Materials & Design, vol. 210, p. 110056, Nov. 2021, doi: 10.1016/j.matdes.2021.110056.
[39] G. P. Serafeim, D. I. Manolas, V. A. Riziotis, P. K. Chaviaropoulos, and D. A. Saravanos, "Optimized blade mass reduction of a 10MW-scale wind turbine via combined application of passive control techniques based on flap-edge and bend-twist coupling effects," Journal of Wind Engineering and Industrial Aerodynamics, vol. 225, p. 105002, Jun. 2022, doi: 10.1016/j.jweia.2022.105002.
[40] F. P. Moncayo-Matute et al., "Surgical planning and finite element analysis for the neurocraneal protection in cranioplasty with PMMA: A case study," Heliyon, vol. 8, no. 9, p. e10706, Sep. 2022, doi: 10.1016/j.heliyon. 2022.e10706.
[41] X. Wang and B. Song, "Application of bionic design inspired by bamboo structures in collapse resistance of thin-walled cylindrical shell steel tower," Thin-Walled Structures, vol. 171, p. 108666, Feb. 2022, doi: 10.1016/j.tws.2021.108666.
[42] B. J. Shelp, E. J. Flaherty, W. J. Sutton, L. M. Schenck, and J. Aalbers, "Commercial validation of a modified method for delivering low nitrogen, phosphorus, and potassium inputs to greenhouse-grown subirrigated pot chrysanthemums," Canadian Journal of Plant Science, vol. 101, no. 6, pp. 962–966, Dec. 2021, doi: 10.1139/cjps-2020-0294.
[43] M. Hussain et al., "Recent Developments in Coatings for Orthopedic Metallic Implants," Coatings, vol. 11, no. 7, p. 791, Jun. 2021, doi: 10.3390/coatings11070791.
[44] J. Ke and Y. Yoshikuni, "Multi-chassis engineering for heterologous production of microbial natural products," Current Opinion in Biotechnology, vol. 62, pp. 88–97, Apr. 2020, doi: 10.1016/j.copbio.2019.09.005.
[45] J. Jacob and S. Bozkurt, "Automated surgical planning in spring-assisted sagittal craniosynostosis correction using finite element analysis and machine learning," PLOS ONE, vol. 18, no. 11, p. e0294879, Nov. 2023, doi: 10.1371/journal.pone.0294879.
[46] R. K. Et. al., "Finite Element Analysis of Honeycomb Sandwich Composite Structures With Various Joints," Turkish Journal of Computer and Mathematics Education (TURCOMAT), vol. 12, no. 1S, pp. 531–535, Apr. 2021, doi: 10.17762/turcomat.v12i1s.1922.